JOURNAL OF MATERIALS SCIENCE 26 (1991) 5127–5133

A review

Microparacrystals: the intermediate stage between crystalline and amorphous

A. M. HINDELEH
Polymer Physics Research Laboratory, Department of Physics, University of Jordan, Amman, Jordan

R. HOSEMANN
Institut für Kristallographie, Freie Universität Berlin, Takustrasse 6, D-1000 Berlin 33, FRG

It has been established that "microparacrystals" are the building blocks of materials in the intermediate stage between crystalline and amorphous. A simplified review of the Theory of Paracrystallinity will be given. The analytical procedure for the determination of the paracrystalline distortion parameter, g_{hkl}, and evidence of the existence of paracrystalline structure in various types of materials will be included. g-values > 0 and $< 15\%$ characterize the world of paracrystalline materials, which range from catalysts ($g \simeq 1\%$) to polymers ($g \simeq 3\%$), graphites ($g \simeq 6\%$), glasses ($g \simeq 12\%$) and molten metals ($g \simeq 15\%$). Extensive studies of g and $\bar{N}$, the average number of netplane layers which build up the paracrystal, have led to a fundamental empirical relation $\alpha^* = \bar{N}^{1/2} g \simeq 0.15$. This relation implies physically that the growth of paracrystals in a particular material is controlled appreciably by the level of g in the netplane structure. Examples on the impact of g on the behaviour of materials will be given. Relationships between g, the crystallinity, and the mechanical properties in polymers will be discussed. The results of our recent investigations on high-modulus Kevlar fibres will be used to demonstrate these relationships.

1. Introduction

X-ray diffraction (XRD) patterns can be discrete spots or lines, traditionally indicative of the so-called "crystalline" structure, or diffuse with broad bands, called "amorphous", "smectic", etc. XRD diagrams of more than a hundred substances, obtained over many years of investigation, proved that matter, in the intermediate stage between amorphous and crystalline, shows certain crystallographic order named by us "paracrystallinity". Expressions like "nodules", "globules", "entanglements", "micells", "meander cubes", "liquid crystals", "amorphous phases", "quasi-crystals", etc., were used by many workers to describe the non-crystalline state. The Theory of Paracrystallinity was introduced in 1950 [1–3], and has been applied successfully to the study of the structures of many types of substances including polymers, biological materials, colloids, catalysts, glasses, metals and melts. Describing it in simplified words, the Theory teaches that both types of XRD patterns, qualitatively indicative of the crystalline and amorphous structures, may reveal, after adequate analysis, an intermediate "paracrystalline" structure, which differs from the other structures solely by the magnitude of the lattice paracrystalline distortion parameter, g, in the substance. If $g < 3\%$, the diffraction pattern is apparently crystalline, whereas if $g > 10\%$ it is apparently amorphous. Quantitative studies proved that even SiO_2 glass and molten metals, with $g = 12\%$ and 15%, respectively, contained microparacrystals [4, 5].

There has been real continued interest in the concepts of intermediate stages between the crystalline and amorphous structures in condensed matter, and in the relationships of the intermediate paracrystalline stages to the properties of the materials. Research workers from various disciplines of science are finding the concept of "paracrystallinity" interesting and appealing, and that it can serve to distinguish various forms of matter. We shall present a short review of the Theory of Paracrystallinity, explain the analytical evaluation of the paracrystalline distortion parameter, g, and provide examples where the Theory of Paracrystallinity has been valuable in the interpretation of the structure and behaviour of materials.

2. Paracrystallinity

The world of noncrystalline matter gave rise to a new mathematical language in the Theory of Paracrystallinity. Without starting from models, the Theory used generalized theoretical concepts and combined them to arrive at its own formulations. Starting from the concepts of von Laue [6] on ideal unbounded lattices, with equidistant netplanes, with the atoms arranged in straight rows and lines and leading to an unbounded "long distance order", the Theory of Paracrystallinity

0022–2461/91 $03.00 + .12

combines this with Debye's concept [7] that each atom in a melt has the same "a priori distance statistics" to its neighbour. Debye applied his idea to isotropic liquids which led to the calculation of the "radial distribution function (RDF)" of atoms in a liquid from XRD analysis. In the Theory of Paracrystallinity, Debye's idea was introduced to the perfect three-dimensional lattice by giving each of the three lattice cell vectors, $\boldsymbol{a}_i$, its own "a priori" distance distribution function, $H_i(x)$, which offers the probability that $\boldsymbol{a}_i$ has the special value $\boldsymbol{a}_i = \boldsymbol{x}$. Nine new statistical quantities g_{ik} were introduced in the crystalline concept (see Fig. 1), which describe by means of the "coordination statistics $H_i(x)$" the relative statistical fluctuations, g_{ik}, of $\boldsymbol{a}_i$ in the direction of $\boldsymbol{a}_k$, and expressed as

$$g_{ik} = \frac{\Delta \boldsymbol{a}_{ik}}{\boldsymbol{a}_k} \tag{1}$$

If g_{ik} is zero, it leads back to the crystallography of the so-called "perfect, or distortion-free crystal". The world of noncrystalline matter gives rise to a wide range of g values > 0 as shown in Table I, that is, intermediate paracrystalline stages between amorphous and crystalline define the world of noncrystalline matter.

Each fundamental physical theory stands on a mathematical language which explains its statements quantitatively. Thus, Maxwell created the language of electrodynamical fields, Minkowski and Einstein defined the four-dimensional imaginary room, and Planck and Schrödinger formulated the guiding waves in atoms with the help of the so-called wave mechanics. The mathematical language adequate to the Theory of Paracrystallinity is based on Ewalds' concept of three-dimensional reciprocal space [8] which is expanded by the vector $\boldsymbol{b}$. The diffraction pattern is described quantitatively in this $\boldsymbol{b}$-space. The integral equations of the Fourier transform and Fourier inverse transform, as well as the convolution (folding) products, squares and convolution polynoms either in the $\boldsymbol{b}$- or $\boldsymbol{x}$-space take care of the clear mathematical language of paracrystallinity.

The paracrystal theory is based on a three-dimensional convolution polynom of distance statistics $H_i(x)$, $(i = 1, 2, 3)$ in the physical space x whose Fourier transform is the "lattice factor $Z(\boldsymbol{b})$" of the microparacrystals. For $g = 0$, $Z(\boldsymbol{b})$ degenerates to the lattice factor of conventional crystallography. By convolution with the shape factor $S^2(\boldsymbol{b})$ of paracrystals it leads to the essential details of the line profiles of reflections. The integral widths, δb, of the reflections depend on the mean number of netplanes, $\bar{N}$, and their relative paracrystalline distance fluctuation, g, and are proportional to h^2, where h is the order of reflection

$$\delta b = 1/\bar{D} + [(\pi g h)^2/\bar{d}] \tag{2}$$

In terms of the netplane spacing d, g can be expressed statistically as follows

$$g = (\overline{d^2}/\bar{d}^2 - 1)^{1/2} \tag{3}$$

In crystallographic terms

$$g_{hkl} = (\overline{d^2_{hkl}}/\bar{d}^2_{hkl} - 1)^{1/2} \tag{4}$$

where hkl are the Miller indices.

The concept of the paracrystal can be well exemplified by the model shown in Fig. 2, which simulates a paracrystal in two dimensions built up of 169

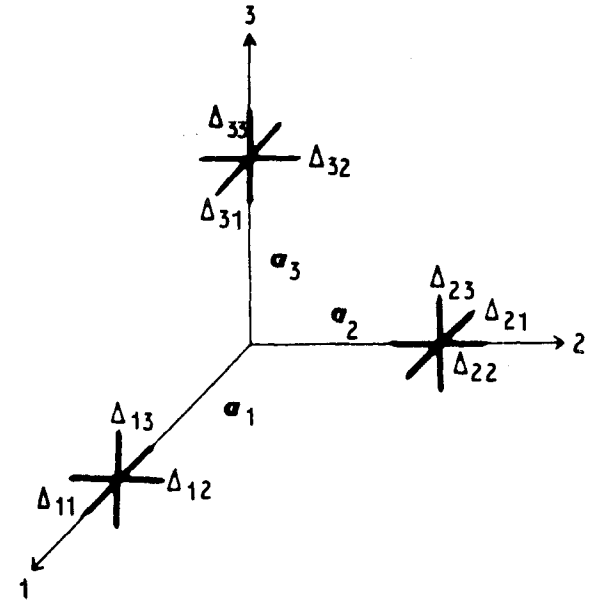

Figure 1 The statistical fluctuation, Δa_{ik}, of three distance vectors $\boldsymbol{a}$ in an orthorhombic paracrystalline lattice.

TABLE I Microparacrystals constituting an intermediate stage between crystalline and amorphous

g (%)	Microparacrystals
0	Crystals
1	Ammonia catalysts
2	So-called "single crystals" of polymers
3	Bulk polymers, biopolymers
6	Graphite of tar coal
12	SiO_2 glass
15	Molten metals
100	Boltzmann gas

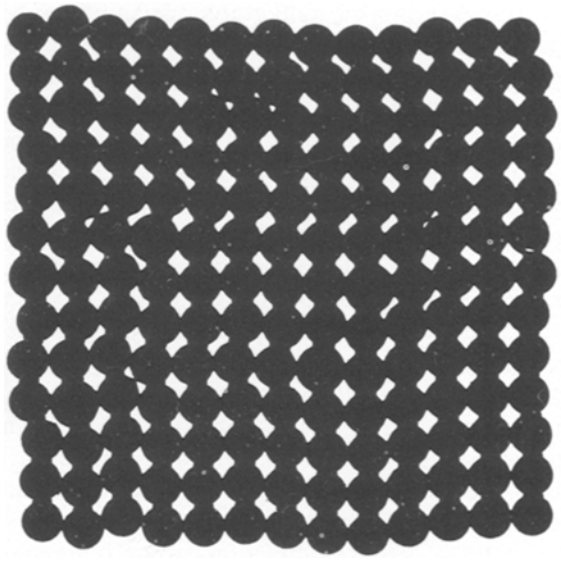

Figure 2 Simulation of a paracrystal in two dimensions using coins of different diameters as point lattices.

coins as lattice points touching each other in four directions; 9 large coins of diameter $D_L = 19$ mm are mixed statistically with the remaining 160 smaller coins of diameter $D_s = 16$ mm. Consequently, the lattice will be paracrystalline-disturbed, that is, the lattice planes now are distorted and statistically curved. The central region of this configuration is relatively better ordered, while larger distortions occur in the outer planes. The mean distance, $\bar{D}$, from centre to centre of adjacent coins is given by

$$\bar{D} = \gamma_s D_s + \gamma_L D_L = 16.1 \text{ mm} \quad (5)$$

where

$$\gamma_s = 160/169 \quad (6a)$$

and

$$\gamma_L = 9/169 \quad (6b)$$

Then g will have the following value

$$g = (\gamma_s \gamma_L)^{1/2} \left(\frac{D_L - D_s}{\bar{D}} \right) = 0.042 \text{ or } 4.2\% \quad (7)$$

It should be made clear that this coin model shows absolutely no statistical correlation between the distance from centre to centre of adjacent coins. The statistical curvature of the netplanes is caused by statistical correlations between neighbouring netplanes with distance statistics expressed by Equation 3. In three-dimensional structures, we are concerned in the value of the fluctuations in the hkl netplanes, which is expressed by Equation 4, and can be determined experimentally by line-profile analysis of the wide-angle XRD, electron diffraction or neutron diffraction as will be discussed in the next section.

3. Analytical determination of g

According to the Theory of Paracrystallinity, the integral breadth, δb, of successive orders of reflection, h, increases linearly with h^2 as shown in Fig. 3. Hence, in the case of the availability of three values of δb measured from three orders of reflections, for example $h = 1, 2, 3$, one can plot δb versus h^2. If the material under investigation is paracrystalline, the three data points will lie on a straight line as illustrated in Fig. 3. The intercept of the line with the ordinate gives the value $(1/\bar{D}_{hkl})$, where $\bar{D}_{hkl}$ is the mean true paracrystal thickness (size) normal to the hkl netplanes. The paracrystalline distortion parameter, g, can be determined from the slope of the line $(\pi^2 g^2/\bar{d})$ and Equation 2. The mean number of netplane layers, $\bar{N}$, is, in fact, $\bar{D}/\bar{d}$ where $\bar{d}$ is the netplane distance. It is worth emphasizing at this stage that an appropriate correction of δb for instrumental broadening effects should be made; details have been discussed earlier [9–13].

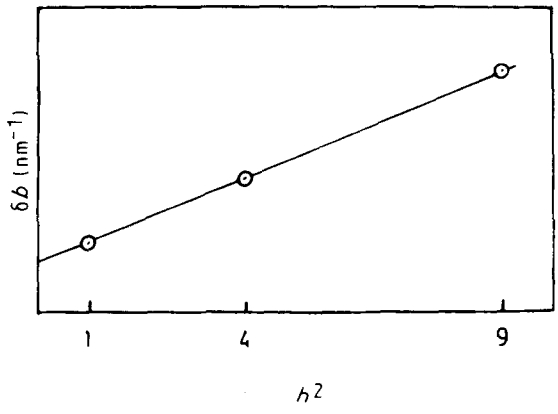

Figure 3 An illustration of δb–h^2 curves for the determination of the true paracrystal size $\bar{D}$, the number of netplane layers $\bar{N}$, the paracrystalline distortion parameter g in paracrystalline substances.

This technique has been applied successfully to the analysis of more than one hundred substances (see, for example, [5, 14–19]). Apart from the highly-crystalline graphite whisker in the form of fibrous polymer with $g \sim 0$ [9], all the other tested samples from various types of materials revealed a paracrystalline structure with g-values ranging from 0.6%–15% as shown in Table I.

4. The α^* law

The application of the Theory of Paracrystallinity to catalysts, biopolymers, fibres, synthetic polymers, glasses and melts led to an empirical relation of a new kind of equilibrium state

$$\bar{N}^{1/2} g = \alpha^* \qquad \alpha^* = 0.15 \pm 0.05 \quad (8)$$

This equation implies that there is a limit to the growth of paracrystal layers, $\bar{N}$, depending on the level of the paracrystalline distortion parameter, g. Fig. 4 shows a plot of $\bar{N}^{1/2}$ as a function of $1/g$ for several substances, and proves that nearly all the paracrystalline samples, independent of their chemical compositions, have led to Equation 8.

Equation 8 also reveals a new physical fundamental law of colloid science, established by a generalized thermodynamics: if atoms or molecules aggregate to condensed matter, then some energy, the so-called surface free energy, is needed at the beginning in order to form the bodies. After a critical size has been reached, the attractive force between the atoms automatically takes care of further growth if undistorted even netplanes are formed into crystals. If the lattice bricks, on the other hand, have different sizes and shapes, and are mixed statistically, then their mutual distances are governed by a priori distance statistics and a paracrystalline lattice grows. Each added netplane produces the same "crystallization heat", the so-called volume enthalpy, by radial attraction forces. On the other hand, the position of the atoms within the nth netplane fluctuates statistically by $n^{1/2}g$ as shown in Fig. 5. The lattice cells, therefore, become more and more angle-distorted with rising values of the square root of the number, n, of the intermediary netplanes, although the lattice bricks preserve the same a priori distance distribution, $H_i(x)$, of their neighbours. With crystal growth, more energy is consumed by the netplanes in order to build up such angle-distorted network, the so-called tangential enthalpy, whilst the crystallization heat of the approaching atoms with their constant a priori distance statistics remains the same. The growth takes place as long as this heat energy is strong enough to overwhelm the tangential

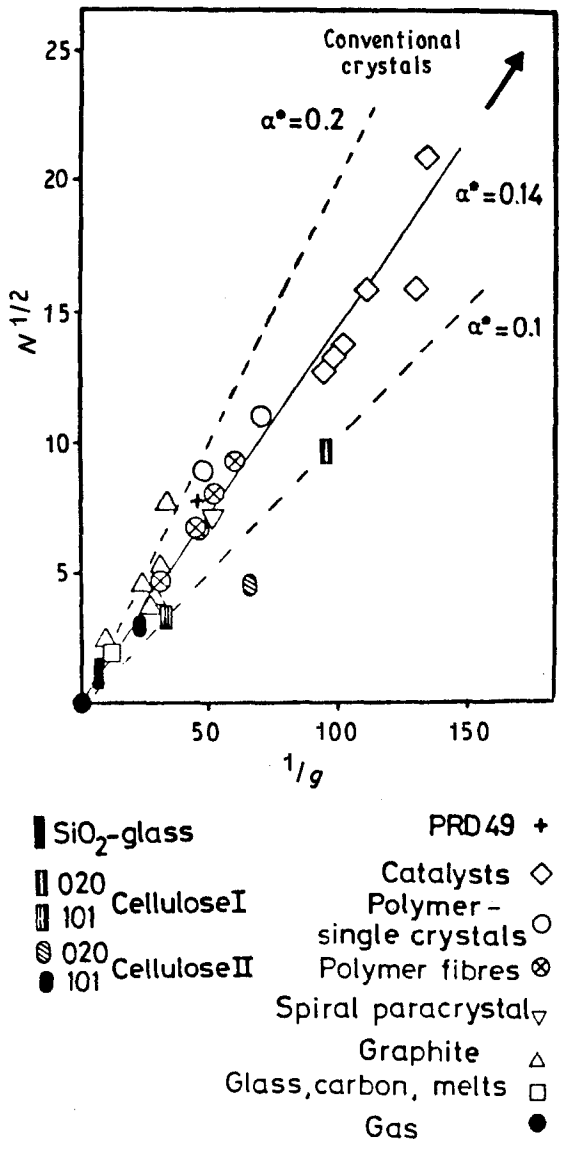

Figure 4 Plot of the square root of $\bar{N}$ against $1/g$ for several paracrystalline substances.

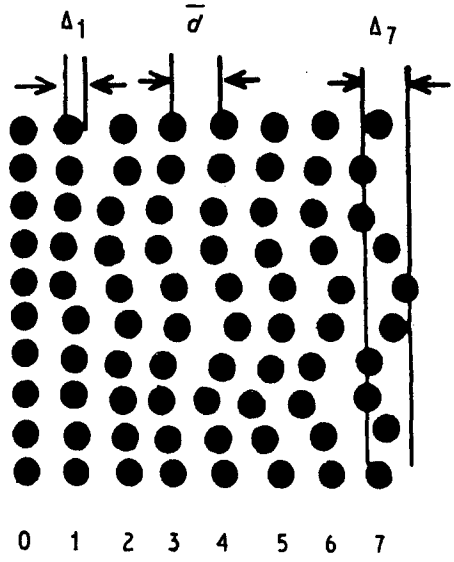

Figure 5 Schematic drawing of paracrystalline distance fluctuations increasing with the square root of the number n of intermediary netplanes.

atom potentials belonging to the distorted values of the bond angles. But, as soon as n reaches the value which satisfies Equation 8, the growth stops and the microparacrystal has reached the thermodynamic new equilibrium state unknown in conventional solid state physics.

The Theory thus detected a new term, ΔG_p, in the thermodynamical enthalpy in addition to the well known surface free energy and volume enthalpy, ΔG_v, of the crystallization heat [5]. In cubic microparacrystals with N^3 lattice cells, the volume enthalpy is given by $N^3 \Delta G_v$ and the paracrystalline tangential enthalpy by $\Delta G_p = 3/2N^4 A_0 g^2$, where A_0 is the coefficient of the atomic tangential potential [18]. The former is exothermic, hence negative, the latter is endothermic, hence positive. Their sum leads to the minimum given in Equation 8. This α^* relation represents the minimum enthalpy, which defines the equilibrium state of microparacrystals. The generalized enthalpy has for $g \neq 0$ a minimum at $N = (\alpha^*/g)^2$ with $\alpha^{*2} = [1 + (1 - 4g^2/\beta)^{1/2}]$, where $\beta = \Delta G_v / 4A_0$. This α^* relation is a thermodynamically founded law; it depends somewhat on g, but also, to an appreciable extent, on the quotient of the volume enthalpy, ΔG_v, and A_0, hence, on the radial atomic potential and tangential potential [18].

5. Experimental evidence of paracrystallinity in matter

Much experimental evidence for the existence of microparacrystals in matter has been obtained in our laboratories and elsewhere; typical examples will be given here.

XRD diagrams obtained by Hosemann *et al.* proved the existence of paracrystalline structure in Fe–Al alloy with $g = 0.6\%$ [20], and in vitreous silica with $g = 12\%$ [4]. Burian *et al.* [21] investigated the structure of evaporated amorphous CdAs films and reported a paracrystalline model of structure. An interesting case was found by Hosemann and Steffen [22] in the paracrystalline structure of liquid lead, which consists of 1 nm large face-centred microparacrystals with $g = 1.5\%$; some of these approximately face-centred liquid-like cells of microparacrystals may convert, within the larger paracrystalline distortion, to icosahedral or icosahedral-like shapes. They undoubtedly are oriented to each other but have nothing to do with the so-called "oriented icosahedra joined at random on their faces" [23]. Morlin *et al.* [24] studied the XRD line profiles of pure and doped, i.e. deformed, alkali halide single crystals and showed that heavily doped NaCl, $CaCl_2$ and $NaCl \cdot NiCl_2$ crystals yielded a number of paracrystalline peaks. Zei [25] suggested a paracrystalline distorted body-centred tetragonal lattice in liquid rubidium. Evidence of paracrystalline structure was found also in the following catalysts: $Cu/Zn/Al_2O_3$ for methanol synthesis [26], $Ni–Al_2O_3$ [27–29], Ni-silica [30], Al_2O_3, dissolved in Fe_3O_4 [31], and $Fe–Al_2O_3$ for ammonia production [26, 30, 32, 33]. Wright *et al.* [27] analysed neutron diffraction profiles and assessed the existence of paracrystallinity in the $Ni–Al_2O_3$ catalyst and obtained $g < 1\%$. In the

field of biology, for example, XRD studies made by Kuckuk and Hosemann [34] revealed $g = 1.5\%$ in ribosome solution. Wheeler and Lewis [35] found that the apatite content of untreated mature cortical bovine bone has $g = 1.5\%$ for the basal plane and 2.9% for the prism plane. In the field of fibrous polymers, the XRD assessments of the paracrystalline structure are numerous, (see, for example [36–40]), and in most cases $g \sim 3\%$, as shown in Table I.

Some specimens of carbon fibres gave several orders of 0 0 1 in the electron diffraction patterns. Curve (a) in Fig. 6 is a plot of the integral breadth against h^2 from the skin of a high-modulus sample with $g = 2\%$ [9]; other specimens gave an average g value of 0.6% in the skin of the carbon fibre and 1.6% in the core [41]. An exceptional case was found in a perfectly ordered sample of a graphite whisker with $g \sim 0$; Curve (b) in Fig. 6 shows a plot of the integral breadth against h^2 for the 0 0 1 electron diffraction profiles of the graphite whisker.

6. Modification of the paracrystalline structure

An interesting example of the possibility of modifying the paracrystalline structure was found recently in Kevlar fibres spun from the polymer poly(*p*-phenylene terephthalamide): Hindeleh *et al.* reported $g = 5.9\%$ for Kevlar 29 fibres [42] and 2.8% for Kevlar 49 fibres [19]. After annealing the fibres in the temperature range from 100–400 °C, g decreased and the crystallinity increased. Above 400 °C, degradation began and consequently g increased and the crystallinity decreased. The α^*-value of the untreated Kevlar 29 [42] was 0.51, which is larger than the normal range given in Equation 8, namely 0.15 ± 0.05. After annealing the fibres at 400 °C, α^* became 0.22; this was explained on the basis that the microparacrystals of Kevlar 29 were not in an equilibrium state when they were initially produced [43]. The untreated Kevlar 49 had $\alpha^* = 0.35$ [19], which decreased to 0.24 after annealing at 400 °C. Such results demonstrate clearly the possibility of modifying the level of the paracrystalline distortion within microparacrystals by appropriate procedures.

Possible structural modifications in copolymers have been reported recently by Johnson *et al.* [44]: poly(*p*-oxybenzoate-co-*p*-phenylene isophthalate) (50/50) and (67/33) fibres spun from nematic mesophase lacked crystalline order. Heat treatment of the fibres resulted in a mosaic of thin "crystalline" regions consisting of *p*-phenylene isophthalate sequences in a paracrystalline matrix.

Interesting examples on the relation between the paracrystalline distortion parameter (g) and the "crystallinity" of polymers are shown in Figs 7 and 8. Fig. 7 shows the inverse relationship between g and the crystallinity in Kevlar 49 fibres, and proves that the "crystallinity" in a paracrystalline material can be considered as a measure of the "degree of perfection" of the lattice netplanes [19, 45, 46]. This proof is supported further by the lattice fringe images obtained by high-resolution electron microscopy and published by Dobb *et al.* [47, 48]. Their diagrams reveal the well-ordered lattice in the organic fibre PRD 49 fibres with $g = 2\%$ [49]; Dobb *et al.* also reported that the lattices of the (1 1 0) and (0 0 2) netplanes are in the form of an array of almost parallel fringes, but in rare cases slightly curved lattices were observed.

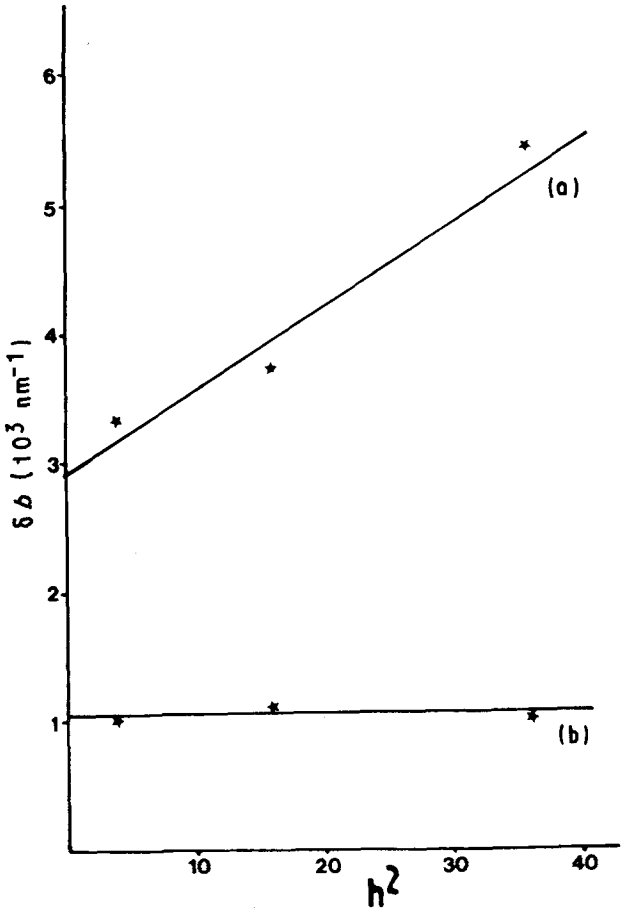

Figure 6 Integral breadth against h^2 for the 0 0 1 reflections of (a) carbon fibre, and (b) graphite whisker [9].

7. The impact of paracrystalline structure on properties

Among the structure–property relationships the following examples will demonstrate clearly the impact

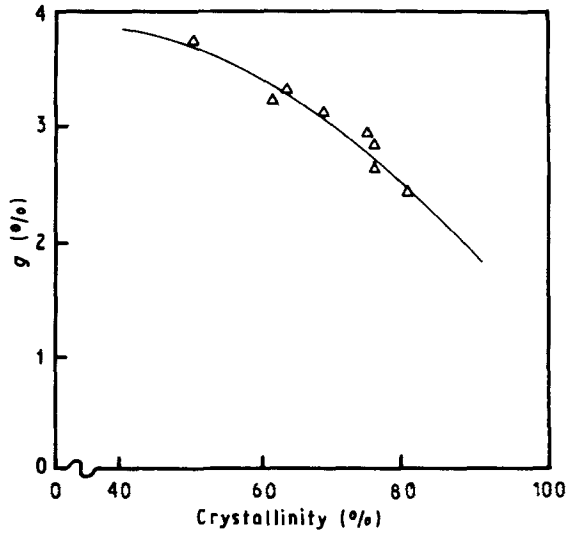

Figure 7 The relationship between g and the crystallinity in Kevlar 49 fibres [38].

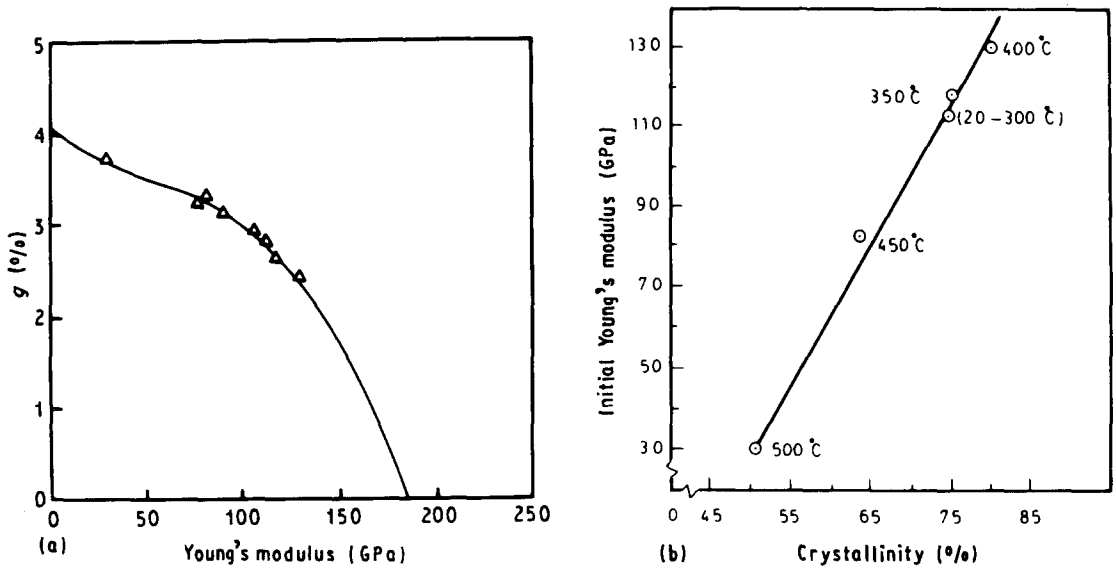

Figure 8 (a) The relationship between g and the Young's modulus in Kevlar 49 fibres [46]. (b) The relationship between the crystallinity and Young's modulus in the annealed Kevlar 49 fibres [53].

of the paracrystalline structure on the behaviour of some materials. Fischer *et al.* [26] reported that the important functions of paracrystallinity in the catalysts are the thermostability of the large inner-surfaces and the improvement of specific surface reactivity. Moreover, it was demonstrated by Fischer *et al.* [26], Fagherazzi *et al.* [33] and Perniconne *et al.* [50] how, owing to paracrystallinity, the specific activity of iron in ammonia synthesis increased about three times after the introduction of alumina. Schultz [51] reported that the paracrystallinity in the catalyst crystals may stabilize them against sintering. Borghard and Boudart [31] mentioned that textural promotion of iron catalysts, that is maintenance of high specific areas of reduced iron samples, was achieved by Al_2O_3 dissolved in Fe_3O_4 prior to reduction; the g value for 10% Al_2O_3 in Fe_3O_4 was 0.6. Wheeler and Lewis [35] found that bone apatite fulfils its biological role of calcium ion control only because it is built up by paracrystals. Saunders *et al.* [52] found a paracrystalline protein, actin, in the stereocilia and cuticular plate region of the hair cell; the paracrystalline array of actin and its cross bridges contributed rigidity and stiffness to the stereocilia.

An interesting relationship between the paracrystalline distortion parameter, g, and Young's modulus in polymers is illustrated in Fig. 8, which is related to Kevlar 49 fibres. Fig. 8a proves that the modulus increases when the distortion parameter g decreases, that is when the lattice structure becomes better ordered [46]; "better ordered" implies higher crystallinity as indicated in Fig. 7. Hence, Fig. 8b proves that the modulus increases when the crystallinity increases [53]. Hindeleh and Abdo [46, 53] obtained, from Fig. 8a and b, modulus values of 185 and 194 GPa at $g = 0$ and crystallinity = 100%, respectively. These results support the theoretical values (180–200 GPa) of the crystal modulus of poly(*p*-phenylene terephthalamide), Kevlar fibres, reported by Fielding-Russel [54] and Tashiro *et al.* [55].

8. Conclusion

Apart from the highly crystalline graphite whiskers in the form of fibrous polymer with $g \sim 0$, all the other tested samples from several types of material revealed a paracrystalline structure with g-values ranging from 0.6%–15%. Moreover, apart from the untreated Kevlar 29 and Kevlar 49 fibres, which had high α^*-values, the other examined materials had α^*-values within the normal range given in Equation 8 and illustrated in Fig. 4, namely 0.15 ± 0.05.

We have demonstrated some important aspects of paracrystallinity, namely (a) how the level of g can be modified by physical means, for example, heat treatment, (b) the relationship between g and the crystallinity in polymers, and that the term "crystallinity" in a paracrystalline material can be considered as a measure of the "degree of perfection" of the lattice netplanes, and (c) the findings of some workers in different fields about the impact of g on the behaviour of matter.

The experimental evidence obtained about the paracrystallinity in the various types of substance have proved undoubtedly that "microparacrystals" are the "building stones" in matter, and that they exist in intermediate stages between "crystalline (ordered lattice)" and "amorphous", with a paracrystalline distortion parameter $0 < g < 15\%$.

Acknowledgement

A.M.H. thanks the DAAD Foundation, FRG for supporting this work.

References

1. R. HOSEMANN, *Z. Phys.* **128** (1950) 1.
2. *Idem, ibid.* **128** (1950) 465.
3. R. HOSEMANN and S. N. BAGCHI, "Direct Analysis of Diffraction by Matter" (North-Holland, Amsterdam, 1962) Ch. 9.
4. R. HOSEMANN, M. P. HENTSCHEL, U. SCHMEISSER

and R. BRÜCKNER, *J. Non-Cryst. Solids* **83** (1986) 223.
5. R. HOSEMANN, *Colloid Polym. Sci.* **260** (1982) 864.
6. M. von LAUE, "Röntgenstrahl-Interferenzen", 3rd Edn (Akademie Verlagsges. Frankfurt am Main, 1960) Ch. 3.
7. P. DEBYE, *Z. Phys.* **28** (1927) 135.
8. P. P. EWALD, *Proc. Phys. Soc. London* **52** (1940) 167.
9. A. M. HINDELEH, D. JOHNSON and P. E. MONTAGUE, in "Fiber Diffraction Methods", edited by A. D. French and K. H. Gardner, ACS Symposium Series No. 141, Washington, DC (American Chemical Society, 1980) p. 149.
10. A. M. HINDELEH and D. J. JOHNSON, *Polymer* **13** (1972) 27.
11. *Idem, ibid.* **13** (1972) 423.
12. *Idem, ibid.* **15** (1974) 697.
13. *Idem, ibid.* **19** (1978) 27.
14. W. VOGEL and R. HOSEMANN, *Acta Cryst.* **A26** (1970) 272.
15. F. J. BALTA-CALLEJA and R. HOSEMANN, *J. Appl. Crystallogr.* **13** (1980) 521.
16. R. HOSEMANN, W. SCHMIDT, A. LANGE and M. HENTSCHEL, *Colloid Polym. Sci.* **259** (1981) 1161.
17. R. HOSEMANN, *Physica Scripta* **T1** (1982) 141.
18. R. HOSEMANN, *Progr. Colloid Polym. Sci.* **77** (1988) 15.
19. A. M. HINDELEH, R. HOSEMANN, G. HINRICHSEN and H. SPRINGER, *Polym. Commun.* **31** (1990) 205.
20. R. HOSEMANN, D. BIALAS, A. SCHÖNFELD, W. WILKE and D. WEICK, in "Advances in Materials" (Pergamon Press, Oxford, 1966) p. 81.
21. A. BURIAN, P. LECANTE, A. MOSSET and J. GALY, *J. Non-Cryst. Solids* **90** (1987) 633.
22. R. HOSEMANN and B. STEFFEN, in "Diffraction Studies on Non-Crystalline Substances" (Separatum, Akademiai Kiado, Budapest, 1981) pp. 491–554.
23. M. WIDOM, *Nature* **327** (1987) 19.
24. Z. MORLIN, A. PETER, I. FOLDVARI and A. MECSEKI, *J. Phys. Coll.* **41** (1980) C6513.
25. M. S. ZEI, *Phys. Rev.* **A27** (1983) 515.
26. A. FISCHER, R. HOSEMANN, W. VOGEL, J. KOUTECKY, J. POHL and M. RALEK, in "Proceedings of the 7th International Congress on Catalysts", Tokyo, Part A, edited by T. Seiyama and K. Tonabe (1980) p. 341.
27. C. J. WRIGHT, C. G. WINDSOR and D. C. PUXLEY, *J. Catal.* **78** (1982) 257.
28. D. C. PUXLEY, I. J. KITCHENER, C. KOMODROMS and N. D. PARKYNS, in "Preparation of Catalysts", 3rd Edn, edited by G. Poncelet, P. Grange and P. A. Jacobs (Elsevier, Amsterdam, 1985) p. 237.
29. C. J. WRIGHT and G. CHRISTOPH, in "Proceedings of the 8th International Congress on Catalysts", Vol. III (1984) p. 59.
30. G. GARBASSI, G. FAGHERAZZI and M. CALCATERA, *J. Catal.* **26** (1982) 338.
31. W. S. BORGHARD and M. BOUDART, *ibid.* **80** (1983) 194.
32. R. HOSEMANN, A. PREISINGER and W. VOGEL, *Ber. Bunsenges. Phys. Chem.* **70** (1966) 796.
33. G. FAGHERRAZI, F. GALANTE, F. GARBASSE and N. PERNICONE, *J. Catal.* **26** (1972) 344.
34. E. D. KUCKUK and R. HOSEMANN, *Colloid Polym. Sci.* **259** (1981) 645.
35. E. J. WHEELER and D. LEWIS, *Calcified Tissue Res.* **24** (1977) 143.
36. R. HOSEMANN and M. HENTSCHEL, *Cellulose Chem. Technol.* **19** (1985) 459.
37. J. GROBELNY, M. SOKOL and E. TURSKA, *Polymer* **25** (1984) 1415.
38. M. F. BOTTIN, M. BOUDEULLE and J. GUILLET, *J. Polymer Sci. Polym. Phys.* **21** (1983) 401.
39. J. LOBODA-ČAČKOVIĆ, H. ČAČKOVIĆ and R. HOSEMANN, *Colloid Polym. Sci.* **252** (1974) 738.
40. G. URBANCZYK, R. DOMAGALA and K. KUCHARSKI, *Polim. Tworzywa. Wielkoczasteczkowe* **26** (1981) 120.
41. S. C. BENETT and D. J. JOHNSON, *Carbon* **17** (1979) 25.
42. A. M. HINDELEH, N. A. HALIM and K. ZIQ, *J. Macromol. Sci. Phys.* **B23**(3) (1984) 289.
43. R. HOSEMANN, M. HENTSCHEL, F. J. BALTA-CALLEJA, E. LOPEZ CABARCOS and A. M. HINDELEH, *J. Phys. C Solid State Phys.* **18** (1985) 961.
44. D. J. JOHNSON, I. KARACAN and J. G. TOMMKA, *Polymer* **31** (1990) 8.
45. A. M. HINDELEH and SH. M. ABDO, *Polym. Commun.* **30** (1989) 218.
46. A. M. HINDELEH, *ibid.* **31** (1990) 32.
47. M. G. DOBB, A. M. HINDELEH, D. J. JOHNSON and B. P. SAVILLE, *Nature* **253** (1975) 189.
48. M. G. DOBB, D. J. JOHNSON and B. P. SAVILLE, *J. Polym. Sci. Polym. Symp. Ed.* **58** (1977) 237.
49. A. M. HINDELEH and R. HOSEMANN, *Polymer Commun.* **23** (1982) 1101.
50. N. PERNICONE, G. FAGHERAZZI, F. GALANTE, F. GARBASSI, F. LAZZERIN and A. MATERA, in "Proceedings of the 5th International Congress on Catalysts", Miami, Vol. II (1972) p. 1241.
51. J. M. SCHULTZ, *J. Catal.* **27** (1972) 64.
52. J. C. SAUNDERS, M. E. SCHNEIDER and S. P. DEAR, *J. Acoust. Soc. Amer.* **78** (1985) 299.
53. A. M. HINDELEH and SH. M. ABDO, *Polymer Commun.* **30** (1989) 184.
54. G. S. FIELDING-RUSSEL, *Text. Res. J.* **41** (1971) 861.
55. K. TASHIRO, M. KOBAYASHI and H. TADOKORO, *Macromol.* **10** (1977) 413.

Received 11 July 1990
and accepted 6 February 1991